Jul 1st, 12:00 AM

Modelling external intrusion into water distribution systems

P. A. López

J. J. Mora

V. Fuertes

F. J. Martínez

iEMSs 2008: International Congress on Environmental Modelling and Software
Integrating Sciences and Information Technology for Environmental Assessment and Decision Making
4th Biennial Meeting of iEMSs, http://www.iemss.org/iemss2008/index.php?n=Main.Proceedings
M. Sànchez-Marrè, J. Béjar, J. Comas, A. Rizzoli and G. Guariso (Eds.)
International Environmental Modelling and Software Society (iEMSs), 2008

Modelling external intrusion into water distribution systems

P.A. López[a], J.J. Mora[a], V. Fuertes[a] and F.J. Martínez [a]

[a] Multidisciplinary Center for Fluid Modeling, Polytechnic University of Valencia, Cno. de Vera, s/n, Valencia, Spain (palopez@gmmf.upv.es, josmorod@doctor.upv.es, vfuertes@gmmf.upv.es, jmsolano@gmmf.upv.es)

Abstract: This article describes the representation of pathogen intrusion in water distribution systems through experimental and numerical modelling, in order to study one of the phenomena which can cause contamination of drinking water through leakage inside the networks. This situation can happen when negative pressure conditions are achieved in the system, allowing the entrance of water around a leak and thus generating pathogen intrusion, causing a problem of water quality. The modelling process is based on experimental and computational procedures. On the other hand, we present an analysis of the behaviour of intrusion considering the transportation of pollutant again by means of experimental measurements and computational simulations.

Keywords: Water quality modelling, Pathogen intrusion, Water distribution systems.

1. INTRODUCTION

Water distribution systems usually conduct good quality water, which is considered safe drinking water to supply the population and thus satisfy their basic needs of consumption. Water quality in the system depends on the quality level, habitually controlled by the water treatment plant. Moreover, the time of residence and the state of the pipes (corrosion, biofilms, and substances transported deposition) can modify the main parameters of water quality. In addition, the possible entry inside the system of elements surrounding the main itself (the so called pathogen intrusion) can become an additional problem (Lopez, 2001).

Water quality and hydraulic performance in networks are linked by the intrusion, as leaks represent a potential influx of undesirable substances in the system. Hydraulic performance of the system (relationship between the water produced and consumed) indicates the lost of volume and pressure, related to the sealing and conservation status (Fuertes et al, 2002, 2003). The risk of water pollution is related to several factors. In 1998, a classification of pathogens entry routes was made, focused on the level of risk considering the causes resulting by the intrusion (Kirmeyer et al, 2001). The routes that have high risk were water treatment breakthrough, transitory contamination, cross connection and water main repair/break.

The aim of this contribution is to make an approach to the problem of pollution occouring in water supply systems based on the pathogen intrusion, as it has been mentioned earlier. The modelling of the leakage from hydraulic point of view can be done as an analysis of flow through an orifice (Lopez, 2005), remaining valid in cases of overpressure and depression, which can favour the entrance of pollutants. The leakage flow depends on the differences in pressure, the resistant feature of the structural defect, the pipe material and

kind of defect (May, 1994). All these aspects have been considered to make the models presented here.

2. PHYSICAL AND COMPUTATIONAL MODEL FOR PATHOGEN INTRUSION IN WATER MAINS

2. 1 Introduction

The proposed study over external intrusion is based on two main aspects. On one hand, two sorts of hydrodynamic models (experimental and computational) have been developed. For the experimental model, a prototype was built in laboratory representing the leakage of the pipe with an orifice, placed in the throat of Venturi tube. Numerical modelling simulates the prototype in three dimensions, using a program based on Computational Fluid Dynamics (CFD), which displays the fields of hydrodynamic components. It gets the best calibration set for the prototype by comparing the velocity and pressure fields along the model. The contrast made with both models allows establishing the foundation for further pathogen intrusion simulations occurring in distribution systems.

On the other hand, an analysis of the behaviour of intrusion is presented considering the transportation of pollutant modelled through a conservative parameter, in this case water salinity. By this modelling, the mixture is studied, as well as the diffusion and transport of pollutants from the area of intrusion through the meshed structure of the model.

By both, mathematical and physical models, it is intended to have a better knowledge of quantities that can not be measured, such as velocity fields, aspects of turbulence, pressure fields, concentrations, etc. existing in mixing processes related to external intrusion. Through computational modelling, we want to study conditions under steady state of the leak and the subsequent mixture, entry and diffusion of the pollutant within the pipe to see in detail the phenomenon that occurs and complement the experiences that will be developed in the laboratory.

2.2 The physical Model

In order to represent the studied flows, and the intrusion phenomenon, the first component to be considered here is a suitable assembly developed in the laboratory (Figure 1). It is oriented to calibrate the computational model with a completely controlled experiment in which the measurements can be very precise.

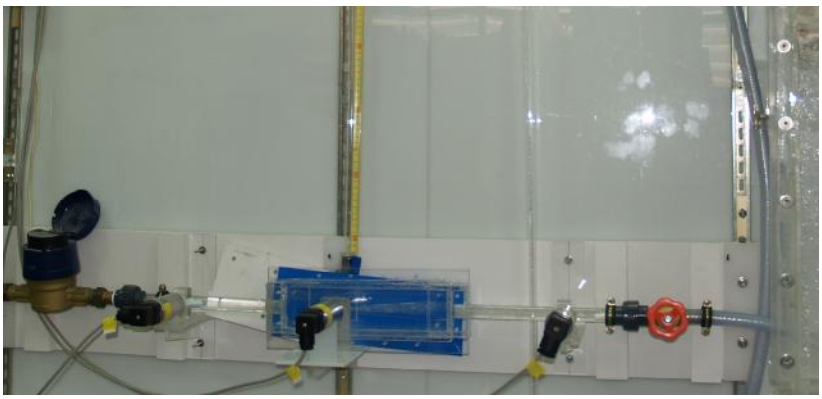

Figure 1. Experimental model for the analysis of the flow into a Venturi tube.

The depression has been represented with a Venturi tube in order to force the intrusion inside the main conduct. Thus, we can observe and model the entrance of external flow inside the principal flow. The Venturi effect is an example of Bernoulli's principle in the case of incompressible fluid flow through a tube or pipe with a constriction. The fluid velocity must increase through the constriction to satisfy the equation of continuity, while its pressure must decrease due to conservation of energy: the gain in kinetic energy is supplied by a drop in pressure or a pressure gradient force. Due to this correlation between the drop of pressure between the zones with different diameters and the circulating volume through the conduit, we can introduce and control de external flow inside the main water flow.

The experiment has been designed to measure pressure and velocity in certain points. A suitable interface has been designed by means of LABVIEW. In Figure 2, a computer screen shows the points in the laboratory assembly where flow and pressure measurements are taken. The intrusion flow was taken in a volumetric way; in each one of the simulations was establish a specific time in order to obtain this intrusion flow.

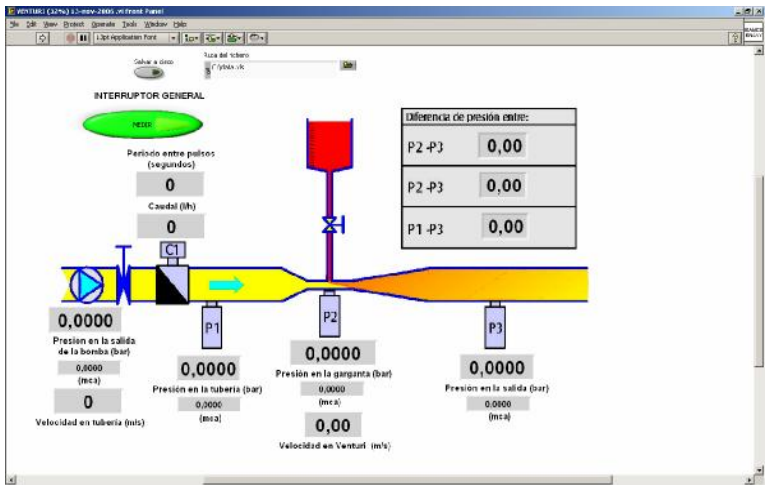

Figure 2. Design of control screen for the measurements in laboratory experience.

In this physical model each measurement was repeated seven times for each one of the nine different apertures of the main valve.

2.3 Computational Model

In order to compare the results of the measurements and to visualize many other aspects, this case has been implemented within the software ©FluentInc. As already indicated, the computational model solves numerically the governing laws of Fluid Dynamics. These equations, taking into account turbulent phenomena, are solved in a geometrical domain, given a number of suitable boundary conditions. In a CFD the relevant magnitudes (velocity, pressure and temperature) are calculated in a discrete manner at the nodes of a certain mesh or grid and they are represented along the mesh.

©FluentInc is a CFD code that uses a numerical method based on the discretization of the space by means of so-called finite volumes (Fluent, 2007) and it offers a number of CFD options for the steady state solution, which can be used in this case. Specifically, incompressible flow and steady state have been considered, together with water as the current fluid under turbulent regime.

The conservation equations solved by the code are those of mass and momentum. The continuity or mass conservation equation solved by ©FluentInc and it is used in the hydrodynamic study of the present problem is the following one:

$$\frac{\partial r}{\partial t} + \nabla r\vec{v} = S_m \quad (1)$$

Where ρ is the fluid density, v its velocity and S_m the mass source contained in the volume of control. For other geometries, suitable coordinates, namely spherical or cylindrical, should be used. Also, the momentum equation is considered by the following expression:

$$\frac{\partial(r\vec{v})}{\partial t} + \nabla r(\vec{v}\vec{v}) = -\nabla p + \nabla \bar{t} + r\vec{g} + \vec{F} \quad (2)$$

Here p is the static pressure, $\vec{g}$ and $\vec{F}$ the gravitational and outer forces defined on the control volume, respectively, and $\bar{t}$ the stress tensor defined by:

$$\bar{t} = m\left[\left(\nabla\vec{v} + \nabla\vec{v}^T\right) - \frac{2}{3}\nabla\vec{v}I\right] \quad (3)$$

Where μ is the eddy viscosity, I is the unit tensor and the third term accounts for the effect of the expansion of volume.

The geometry in study was constructed in AutoCAD® 2006 considering the sections where pressure was measure in the physic model. The mesh was designed on Gambit 2.2.30, in this software it established the volume control and the solid and liquid elements, defining the computational dominium and constructed a *Tgrid* mesh (Figure 3).

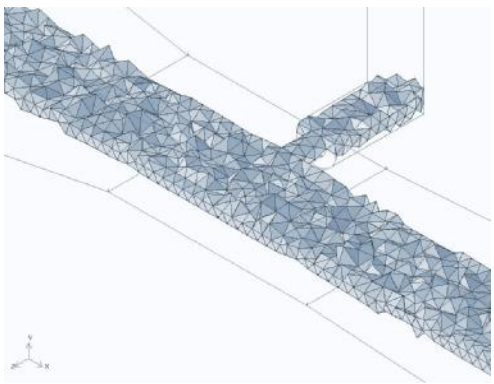

Figure 3. Details of the generated mesh.

Once the mesh has been built and suitably refined for the solution of the equations to be optimal, it is necessary to define the boundary conditions. These conditions must be compatible with the solution strategies of the calculation code.

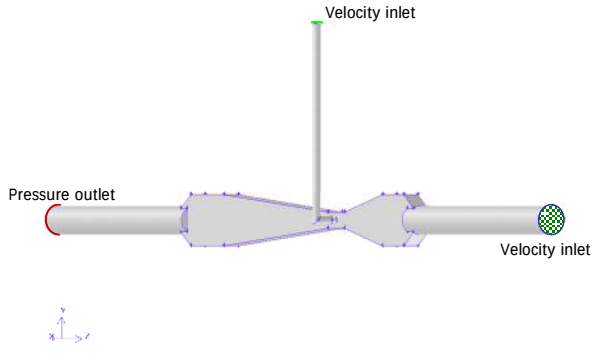

Figure 4. Boundary conditions.

On the ©FluentInc software, the boundary conditions shown in figure 4 were defined. The model works with velocity inlet boundaries at the entry of the flow on principal and intrusion sections; and pressure outlet boundary on the final section of the main tube. The hydraulic diameter method and the turbulence intensity were considered for boundaries.

Focus on the conditions of this model, the *RNG k-e* turbulent model is the best option. It considers in its equations some terms that improve the accuracy for flows that are filtered

rapidly, solve accurately the phenomenon of vortices in the flow, and also manage with differential effective viscosity to consider effects of small Reynolds numbers.

In order to improve the accuracy of the solution, second-order discretization was used for numerical method. The gradient option was modified from cell-based to node-based in order to optimize energy conservation; this option is more suitable for tri-elements meshes (Fluent, 2005). Finally, the calculation made requested approximately 300 iterations for every one of the experimental cases.

3. ANALYSIS OF RESULTS

3.1. Hydrodynamic model analysis

After making the experimental and computer simulations, we show the results which describe the agreement of both models. Table 1 shows the results obtained from the experimental simulation. These data are the necessary information to establish the boundary conditions for the numerical model.

In the Venturi throat section, the pressures were negatives as expected in almost all the different nine experiments for different flows. This forced negative pressure is the cause of the intrusion of flow in the main current.

Table 1. Experimental flows for the different experiments (l/h)

	Principal	Intrusion		Principal	Intrusion
1	341,7	45,4	6	2068,8	50,7
2	540,4	45,4	7	2316,7	53,2
3	1074,4	45,5	8	2548,6	55,9
4	1325,2	46,2	9	2857,1	60,1
5	1828,6	48,1			

Figure 5 shows the contours of velocity and pressure for maximum, intermediate and minimum flow in the intrusion zone. In those figures we can observe that the maximum flow occurs after the intrusion section, this maximum velocity registered on the computational model was 13,42m/s. On the same way the minimum pressure is established just on the corner of the intrusion tube, presenting a negative pressure of -70.000Pa. When the flow is reduced, also the velocity and the pressure tend to zero.

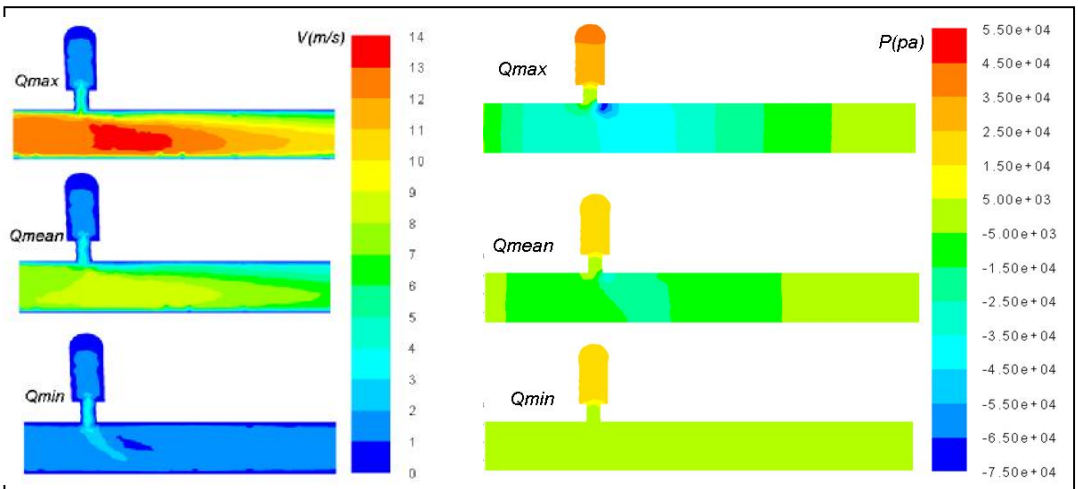

Figure 5. Velocity and pressure fields.

Once the laboratory experiment and the computational model of the problem have been performed, we can analyze both results together. These results, after computational model calibration, are shown in Figures 6 and 7. As it can be seen, the agreement for pressure and velocity values between measured and numerical results is satisfactorily achieved.

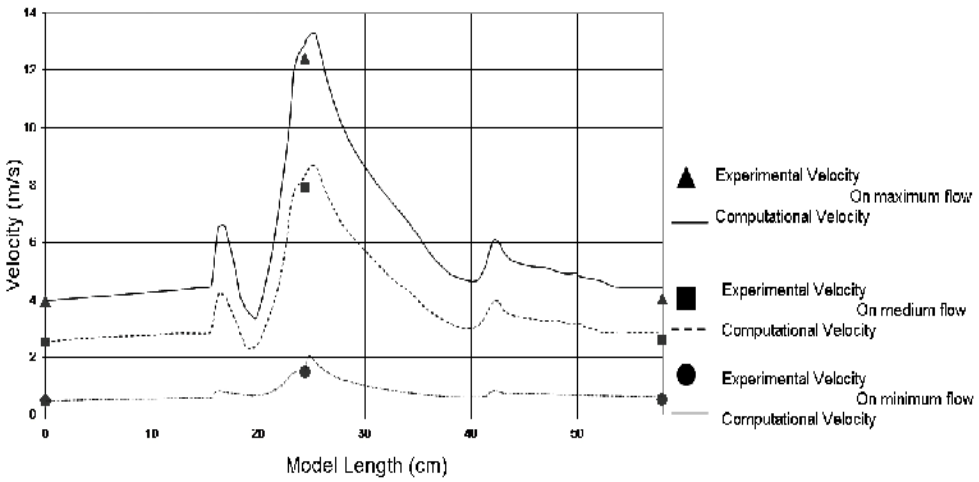

Figure 6. Velocity measurements vs. computational model predictions.

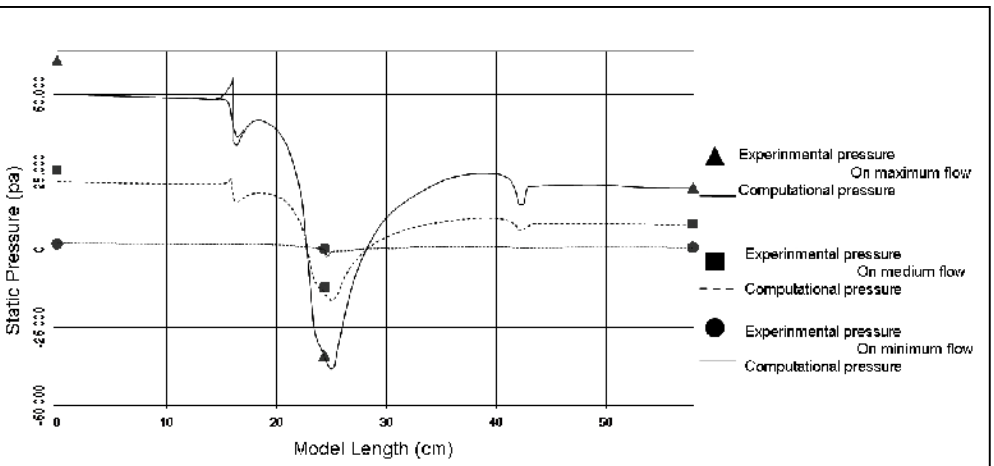

Figure 7. Pressure measurements vs. computational model predictions.

The error was established considering the Nash-Sutcliffe efficiency (*E*), that is one of the most used criteria for the hydrologic evaluation between simulated and observed variables (Krause et al, 2005). It is defined as one minus the sum of the absolute squared differences between the predicted and observed values normalized by the variance of the observed values during the period under investigation. It is calculated as:

$$E = 1 - \frac{\sum_{i=1}^{n} (O_i - P_i)^2}{\sum_{i=1}^{n} (O_i - \overline{O}_i)^2} \qquad (4)$$

With *O* observed and *P* predicted values. The range of *E* lies between 1,0 (perfect fit) and -∞. An efficiency of lower than zero indicates that the mean value of the observed would have been a better predictor than the model. In this case, we assess the velocity and pressure

of both models in every section of measurement. With respect to the velocity configuration, evaluated in the intrusion and the final sections of the models, the results obtained were 0,9883 of similitude from the intrusion section, and 0,9516 on the final section. On the same way, the pressure configuration was evaluated, in this case considering the first section and the intrusion sections of the models, the results were 0,9260 on the first section, and 0,9988 on the intrusion section. All of these results present more of the 92% of similitude between the computational and experimental models. Considering that the predicted values were adequate for the representation of the experimental model.

Computational modelling is consistent with the physical prototype adequate in the flow range considered. This conclusion leads us to consider the computational model as an entity that represents in detail the velocity and pressure fields, in those points where measurements are not available or in points that require contrast.

3.2. Quality model.

Based on the hydrodynamic model of the intrusion, some experiments to represent water quality in the intrusion mixture have been carried out. In this case, water quality intends to be represented through a conservative parameter such as electrical conductivity. A little volume of water with a huge electrical conductivity is used to represent the pollutant intrusion.

The physical experiments were conducted on the following schedule: the principal flow represents a main in the network water and the initial flow rate on the prototype, this higher volume has a low conductance. On the other hand, we represent the flow of intrusion with a small volume but with a high salinity concentration. Finally, we capture the information flow resulting from the mixture. The measurement of the volumetric flow rate of pollutant intrusion was carried out by three tests for each one of the 11 cases modelled for the main flow.

Two different conditions were considered in the mathematical model, first one represents the main flow with a low electrical conductivity; second one represents the flow generated through the intrusion, with a high concentration of salinity and thus a much higher electrical conductivity than that existing in the main flow.

For this case, in order to solve conservation equation for chemical species, ©FluentInc predicts the local mass fraction of each species, Y_i, through the solution of a convection-diffusion equation for the *i*th species (Fluent, 2007). This conservation equation takes the following general form:

$$\frac{\partial}{\partial t}(rY_i) + \nabla \cdot (r\mathbf{v}Y_i) = -\nabla \cdot \mathbf{J}_i + R_i + S_i \qquad (5)$$

Where R_i is the net rate of production of species *i* by chemical reaction and S_i is the rate of creation by addition from the dispersed phase plus any user-defined sources. In turbulent flows, ©FluentInc computes the mass diffusion in the following form:

$$J_i = -\left(rD_{i,m} + \frac{m_t}{Sc_t} \right) \nabla Y_i \qquad (6)$$

Where Sc_t is the effective Schmidt number for the turbulent flow (it varies with the turbulent viscosity, m_t, and the turbulent diffusivity), and $D_{i,m}$ the mass diffusion coefficient for species *i* in the mixture.

To specify boundary conditions, mass flow inlet condition was established for the principal and intrusion entrances. This boundary condition defines both flow and density of water and also the pressure. The density of water was measured in the experimental model in addition of hydrodynamic parameters indicated on the experimental simulations.

Table 2. Input parameters on the numerical model

Simulation	Principal inlet boundary	Instrusion inlet boundary	Oulet boundary
	Mass flow (kg/s)	Mass flow (kg/s)	velocity (m/s)
1	2,86E-05	1,59E-04	0,309
2	5,97E-05	8,36E-05	0,625
3	8,58E-05	1,15E-04	0,898
4	1,06E-04	3,59E-04	1,121
5	1,23E-04	3,78E-04	1,307
6	1,44E-04	3,66E-04	1,517
7	1,61E-04	3,66E-04	1,699
8	2,18E-04	3,01E-04	2,281
9	2,51E-04	3,64E-04	2,629
10	2,76E-04	3,71E-04	2,887
11	3,04E-04	3,80E-04	3,177

We simulated the same conditions established on the hydrodynamic model, the simulations were in steady state and converge were presented between 250 and 300 iterations. As a result we present the mixture in which can observe the percentage of maximum mass flow contaminant of 6,10% in the last section of the model. The configuration of the concentration of contaminant flow can be seen as follows (Figure 8).

Figure 8. Salinity configuration when the percent of max flux contaminated is 6,10% on the output of the model

To calibrate the transport model some comparisons between the theoretical, experimental and computational modelling have been done. The mean absolute error of computational model from the result of theoretical and experimental study is 0,090 and 0,082. The certainty of the computational modelling is 91,0 and 91,8%. Again in this case the agreement between the modelling predictions of the mixture concentration and the theoretical calculations were adequate. The computational model let us visualize the mixture region along the section of the tube.

4. CONCLUSIONS

Contamination of drinking water due to exposure to biological and chemical pollutants is a very important cause of diseases. One of the causes for this sort of water pollution is external intrusion of pathogen agents across defects in the pipes. In this contribution we have studied the phenomenon of external pathogen intrusion in water mains by means of simulation models.

We have developed two ways of solving the problem: by physical prototype and numerical computations; by both mathematical and physical models. We have intended to achieve a better knowledge of quantities that can not be measured, such as velocity fields, aspects of turbulence, pressure fields, concentrations, etc. presented in mixing processes when unusual situations occur in the system.

Through computational modelling, we want to study conditions under steady state of the leak and the subsequent mixture, entry and diffusion of the pollutant within the pipe to see in detail the phenomenon that occurs and complement the experiences that will be developed in the laboratory.

5. ACKNOWLEDGMENTS

This article has been made possible through actions of the CMMF researchers, involved in the following projects: *DANAIDES: Desarrollo de herramientas de simulación para la caracterización hidráulica de redes de abastecimiento a través de indicadores de calidad del agua. REF. DPI2007-63424. Ministerio de Educación y Ciencia de España.*

REFERENCES

Fluent, TUTORIAL 1, Introduction to Using FLUENT: Fluid Flor and Heat Transfer in a Mixing Elbow, © Fluent Inc. January, 2005.

Fluent User Manual. 2007. Internet url: http://www.fluent.com/.

Fuertes, V.S., García-Serra, J., Iglesias, P.L., López, G., Martínez, F.J., Pérez, R., Modelación y diseño de redes de abastecimiento de agua, Fluid Mechanics Group. Polytechnic University of Valence, Spain, 2002.

Fuertes, V.S., Iglesias, P.L., Izquierdo, J., López, P.A., López, G., Martínez, F.J., Pérez, R., Ingeniería hidráulica en los abastecimientos de agua, Fluid Mechanics Group. Polytechnic University of Valence, Spain, 2003.

Kirmeyer, G.J., LeChevalier, M.W., Pathogen Intrusion into Distribution Systems [Project #436], http://www.awwarf.com/exsums/436.htm, American Water Works Association Research Foundation (AWWARF), USA.

Krause, P., Boyle, D. P., Bäse, F., Comparison of different efficiency criteria for hydrological model assessment, Advances in Geosciences, 5, 89-97, 2005.

López, P.A. Metodología para la calibración de modelos matemáticos de dispersión de contaminantes incluyendo regímenes no permanentes. PhD Thesis Disertation, Polytechnic University of Valence, 2001.

López P.A., Fuertes, V., Iglesias P.L., Martínez, F.J., Modelación mediante cfd de fugas en tuberías de redes de abastecimiento. Ponencia en V Seminario Iberoamericano de planificación, proyecto y operación de sistemas de abastecimiento de agua. ISBN 84-89487-20-0 Valence, Spain. December 2005.

May, J. Pressure-dependent leakage, World Water and Environmental Engineering, October 1994.